Am J Physiol Regul Integr Comp Physiol 289: R656–R662, 2005.
First published April 28, 2005; doi:10.1152/ajpregu.00179.2005.

TRANSLATIONAL PHYSIOLOGY

HIV protein, transactivator of transcription, alters circadian rhythms through the light entrainment pathway

J. P. Clark, III,[1] Christopher S. Sampair,[2] Paulo Kofuji,[1] Avindra Nath,[3] and Jian. M. Ding[1,4]

[1]*Neuroscience Program and* [2]*School of Dentistry, University of Minnesota, Minneapolis, Minnesota;* [3]*Department of Neurology, Johns Hopkins University, Baltimore, Maryland; and* [4]*Department of Physiology, Brody School of Medicine, East Carolina University, Greenville, North Carolina*

Submitted 14 March 2005; accepted in final form 27 April 2005

Clark, J. P., III, Christopher S. Sampair, Paulo Kofuji, Avindra Nath, and Jian. M. Ding. HIV protein, transactivator of transcription, alters circadian rhythms through the light entrainment pathway. *Am J Physiol Regul Integr Comp Physiol* 289: R656–R662, 2005. First published April 28, 2005; doi:10.1152/ajpregu.00179.2005.—Patients infected with the human immunodeficiency virus (HIV), and other mammals infected with related lentiviruses, exhibit fatigue, altered sleep patterns, and abnormal circadian rhythms. A circadian clock in the hypothalamic suprachiasmatic nucleus (SCN) temporally regulates these functions in mammals. We found that a secretary HIV transcription factor, transactivator of transcription (Tat), resets the murine circadian clock, in vitro and in vivo, at clinically relevant concentrations (EC_{50} = 0.31 nM). This effect of Tat occurs only during the subjective night, when *N*-methyl-D-aspartate (NMDA) receptor [D-2-amino-5-phosphonovaleric acid (0.1 mM)] and nitric oxide synthase (N^G-nitro-L-arginine methyl ester, 0.1 mM) inhibitors block Tat-induced phase shifts. Whole cell recordings of SCN neurons within the brain slice revealed that Tat did not activate NMDA receptors directly but potentiated NMDA receptor currents through the enhancement of glutamate release. Consistent with this presynaptic mechanism, inhibitors of neurotransmission block Tat-induced phase shifts, such as tetrodotoxin (1 μM), tetanus toxin (1 μM), P/Q/N type-calcium channel blockers (1 μM ω-agatoxin IVA and 1 μM ω-conotoxin GIVA) and bafilomycin A_1 (1 μM). Thus the effect of Tat on the SCN may underlie lentiviral circadian rhythm dysfunction by operating as a disease-dependent modulator of light entrainment through the enhancement of excitatory neurotransmission.

glutamate; phase shift; human immunodeficiency virus

THE BRAIN'S CIRCADIAN CLOCK, the suprachiasmatic nucleus (SCN), imparts daily oscillations in behavioral and bodily functions (27). The SCN possesses an intrinsic rhythm that synchronizes with environmental light-dark cycles (36). During this light entrainment process, light depolarizes retinal ganglion cells that release Glu from their terminals within the SCN (14). Although the SCN is exposed to Glu during daylight hours, the circadian clock can be reset by this neurotransmitter only during the subjective night (11).

Patients infected with HIV and other mammals infected with related lentiviruses exhibit irregularities in circadian rhythms of activity, body temperature, and circulating immune cells that begin around the time of primary infection and progress throughout the course of the disease (2, 4, 23, 42, 44). These circadian abnormalities are coincident with fatigue, declining sleep quality and altered sleep architecture, together implicating pathological changes in the brain's ability to temporally coordinate these functions (10, 31, 37). How lentiviral infections alter sleep and circadian rhythms remains unknown.

Although HIV can only sustain a productive infection in mononuclear phagocytes within the central nervous system (CNS), neuronal dysfunction and, in some conditions, cell death are believed to underlie HIV-induced neurological disorders (18). These infected immune cells initiate lentiviral encephalopathy by secreting viral and/or cellular factors that can lead to Glu receptor activation and neurotoxicity (26, 29). Several HIV proteins can modulate the excitability and viability of neurons (29) and cause comparable cognitive, movement, and sleep disorders to those of lentiviral infection (32, 39).

Of these proteins, transactivator of transcription (Tat) plays an important role in lentiviral neuropathogenesis. Tat is an obligatory transcription factor that is secreted from infected cells into the extracellular space (5) and is internalized rapidly into neighboring cells, where it stimulates viral replication through the HIV promoter (43). Extracellular application of Tat leads to ionotropic Glu receptor activation (7, 16, 30, 41) and induces proinflammatory cytokine production (35), cellular factors that enhance Glu transmission (1). Tat reproduces the encephalopathy of lentiviral infection when it is presented to the CNS, as a secreted or exogenous factor, (3, 17, 19, 35), and this condition is prevented with *N*-methyl-D-aspartate (NMDA) receptor and NO synthase blockers (17).

We hypothesize that sleep and circadian rhythm disorders are caused by alterations in light entrainment, which result from changes in Glu transmission by factors secreted during lentiviral infection. Because Tat is an essential lentiviral transcription factor that contributes to the neurological conditions of infection, we investigated whether Tat could alter the light entrainment pathway.

MATERIALS AND METHODS

Extracellular recordings. Coronal hypothalamic brain slices containing the SCN, 500-μm thick, were prepared from male C57B/6 mice (Charles River, Wilmington, MA; Harlan, Indianapolis, IN), 6–12 wk of age, at least 2 h before the offset of light in the 12:12-h

Address for reprint requests and other correspondence: J. Ding, Associate Professor, Dept. of Physiology, Brody School of Medicine, East Carolina Univ., 600 Moye Blvd., Greenville, NC 27858 (e-mail: deanj@mail.ecu.edu).

The costs of publication of this article were defrayed in part by the payment of page charges. The article must therefore be hereby marked "*advertisement*" in accordance with 18 U.S.C. Section 1734 solely to indicate this fact.

light-dark cycle of the colony chamber. Spontaneous action potentials were recorded with glass electrodes (3–5 MΩ, filled with 5 M NaCl) from the SCN of brain slices maintained in Earle's balanced salt solution supplemented with 24.6 mM glucose, 26.2 mM sodium bicarbonate, 5 mg/l of gentamicin and gassed continuously with 95% O_2-5% CO_2 at 37°C (pH 7.4, Sigma-Aldrich, St. Louis, MO). Action potentials generated from individual neurons were isolated on an oscilloscope with a window discriminator in real time on the basis of amplitude, waveform, polarity and cadence and counted by a customized program (Labview, National Instruments, Austin, TX). Running means were calculated to determine the time of peak activity (12).

During drug treatment, the media level was lowered to expose the surface of the brain slice. Microdroplets (0.2 μl) of agonist were applied, bilaterally, with a microsyringe (Hamilton, Reno, NV) to the SCN at the circadian time indicated (e.g., CT 16) for 10 min. Antagonists were bath applied 20–50 min before the indicated treatment time in addition to the 10-min treatment period (e.g., CT 16–16:10). A three-parameter Hill equation

$$\left(f(x) = \frac{ax^b}{c^b + x^b}\right)$$

was used to fit the data points from the concentration response curves (Fig. 1*C*, Sigma Plot 8.0, SPSS, Chicago, IL) and to derive the concentrations required to elicit a half-maximal phase delay for Tat (EC_{50} = 0.312 nM: a = 3.112, b = 7.94E-1, c = 3.16E-10, r^2 = 0.99) and Glu (EC_{50} = 1.95 mM: a = 3.457, b = 9.06E-1, c = 2.08E-3, r^2=0.99). One-way ANOVA and Scheffé's means comparison procedures were used to evaluate statistical significance of the phase-shifting experiments at an alpha level of 0.05 using Origin 7.0 (OriginLab, Northampton, MA) and Excel (Microsoft, Seattle, WA).

Intracellular recordings. For whole cell patch-clamp recordings, 250- to 350-μm coronal hypothalamic murine brain slices were sectioned before CT 10 on a vibratome in ice-cold, oxygenated (95% O_2-5% CO_2) artificial cerebral spinal fluid (aCSF) (in mM): 130 NaCl, 26 $NaHCO_3$, 3 KCl, 5 $MgCl_2$, 1.25 NaH_2PO_4, 1.0 $CaCl_2$, 10 glucose (pH 7.2–7.4, osmolality 290–305 mosmol). These slices were initially incubated for 20 min at ~36° C and allowed to cool to room temperature (23–25° C) in aCSF (same as above but with 0 mM $MgCl_2$, 2 mM $CaCl_2$). At CT ≥ 13, slices were transferred to a recording chamber mounted on the stage of an upright microscope (E600 FN, Nikon, Tokyo, Japan) equipped with differential interference contrast optics and infrared video imaging system (DIC-IR, Dage-MTI CCD100 Camera, Michigan City, IN), which was used to visualize SCN neurons in the brain slice. Whole cell recordings were made from the soma of ventral-lateral SCN neurons at room temperature (23–25° C) using a multiclamp 700A amplifier (Axon Instruments, Union City, CA) with fire-polished borosilicate pipettes (3–7 mΩ, Sutter Instruments, Novato, CA) filled with (in mM) 125 Cs-methane sulfonate, 4 NaCl, 3 mM KCl, 1 $MgCl_2$, 4 MgATP, 9 EGTA, 8 HEPES, 1 GTP, 0.1 leupeptin, 10 phosphocreatine (pH 7.2, osmolality 290–295 mosmol). These neurons were identified by their high-input resistances (>1 GΩ), sodium channel activation in the absence of tetrodotoxin (TTX) and spherical somas localized superior to the optic chiasm and inferior and lateral to the third ventricle. The recording solution contained (in mM) 0 $MgCl_2$, 10 TEA-Cl, 120 NaCl, 26 $NaHCO_3$, 3 KCl, 1.25 NaH_2PO_4, 1.0 $CaCl_2$, 10 glucose (pH 7.2–7.4, osmolality 290–305 mosmol) supplemented with (in mM) 0.1 picrotoxin, 0.1 NBQX, 0.1 D-serine, 0.01 nifedipine, 0.001 tetrodotoxin. Series resistance and liquid junction potentials (measured to be −4.9 mV) were not compensated. All traces were sampled at 5–10 kHz and low-pass filtered at 2 kHz. SCN neurons were subjected to

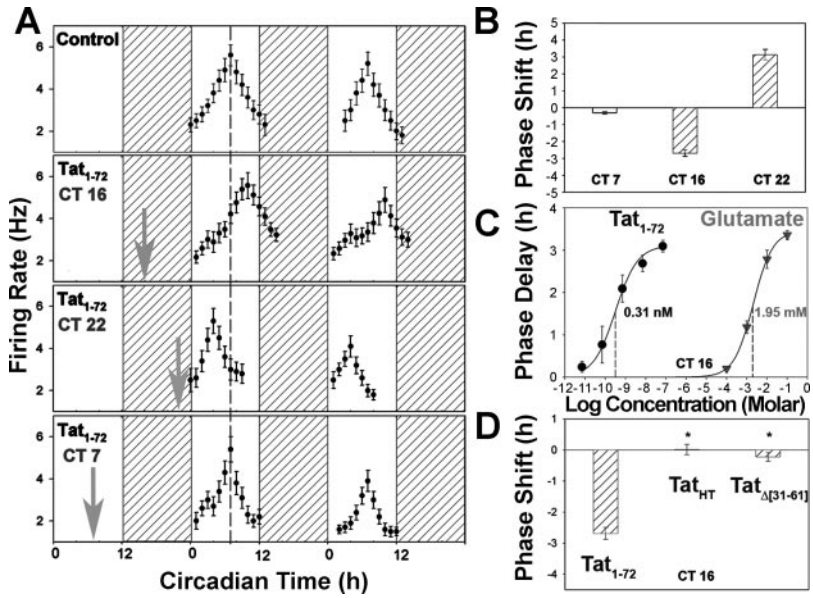

Fig. 1. The first 72 amino acids of transactivor of transcription ($Tat_{1–72}$) reset the circadian clock, in vitro. *A*: the control illustrates the circadian rhythm of spontaneous action potentials recorded from one untreated suprachiasmatic nucleus (SCN) slice on *days 2* and *3*, in vitro. Each time point in this rhythm is an average of firing frequencies (Hz) recorded with single-unit extracellular electrodes within 1 h of the indicated circadian time (CT). SCN application of 7 nM $Tat_{1–72}$ for 10 min (arrows), followed by a buffer rinse, delayed the circadian clock at CT 16, advanced the circadian clock at CT 22, but did not alter the phase of the circadian clock during the midsubjective day, CT 7. (Oblique hatch marks indicate the dark period of the vivarium light-dark cycle, and the dashed vertical line denotes CT 7 on the 2nd day in vitro.) *B*: the bar graph illustrates the average phase shift resulting (means ± SE) from $Tat_{1–72}$ application (0.2 μl, 7 nM for 10 min) at CT 7, 16, and 22, where 0-h phase shift is normalized to the mean control SCN rhythm (6.84 ± 0.08 h, n = 6). *C*: the concentration-response curve resulting from CT 16 SCN applications of $Tat_{1–72}$ and Glu are represented by the mean phase delay (±SE) at the indicated concentrations. A three-parameter Hill equation was used to fit the data points and to derive the concentrations required to elicit a half-maximal phase delay for Tat (EC_{50} = 0.312 nM, r^2 = 0.99) and Glu (EC_{50} = 1.95 mM, r^2 = 0.99). *D*: phase delays after a 10-min application of $Tat_{1–72}$ (0.2 μl, 7 nM, −2.69 ± 0.19 h, n = 8), heat-treated $Tat_{1–72}$ (HT, 70°C for 30 min, 0.01 ± 0.17 h, n = 3) or $Tat_{\Delta[31–61]}$ ($Tat_{1–72}$ with the amino acids 31–61 excised, −0.22 ± 0.14 h, n = 3) at CT 16. Asterisks indicate statistically significant means using Scheffé's post hoc tests (*$P < 0.05$) relative to the $Tat_{1–72}$ condition, following a one-way ANOVA ($P < 0.0001$).

voltage ramps (−70 mV/30 mV/−90 mV/−70 mV in 800 ms/100 ms/50 ms, respectively) every 30 s, and the average of three traces was monitored in pClamp 8.0 (Axon Instruments) and analyzed on-line with ClampFit 8.0 (Axon Instruments) and Excel. For some experiments, NMDA receptor currents were evoked with biphasic pulses (0.4 ms, 25–125 μA, at 0.2 Hz) from a bipolar electrode positioned on the optic chiasm and driven by a stimulus isolator (Model A360, World Precision Instruments). Stimulus-evoked NMDA currents were recorded at a holding potential of −70 mV and averaged (n = 10) in a recording solution containing (in mM) 0 $MgCl_2$, 130 NaCl, 26 $NaHCO_3$, 3 KCl, 1.25 NaH_2PO_4, 2.0 $CaCl_2$, 10 glucose (pH 7.2–7.4, osmolality 290–305 mosmol) supplemented with 0.1 picrotoxin and 0.01 NBQX. To improve the voltage clamp in these experiments, recording pipettes were filled with (in mM): 125 Cs-methanesulfonate, 4 NaCl, 1 $MgCl_2$, 4 MgATP, 9 Cs-BAPTA, 8 HEPES, 1 GTP, 0.1 leupeptin, 10 phosphocreatine, 3 QX-314 (pH 7.2, osmolality 290–295 mosmol). Paired t-test procedures were used to evaluate statistical significance of evoked NMDA current recordings. The statistical procedures were executed in Origin and MS Excel using an alpha level of 0.05.

In vivo experiments. Guide cannulas (22-gauge with 28-gauge stylet, AP 0.4 mm, LM 0.1 mm, DV 4.0 mm) were stereotaxically implanted to the SCN of anesthetized (ketamine/xylazine, 40/4 mg/kg ip), male mice (129/B6, 20–25 g, 6-wk-old; Charles River). Postsurgery mice were individually housed in cages equipped with 6-inch running wheels for at least 10 days in 12:12-h light-dark cycle before their release into constant darkness (DD). Wheel-running activity was monitored in 5-min intervals on a Pentium computer equipped with Vital View 3.11 data acquisition software (Minimitter, Sunriver, OR). The injection times (CT 16) were calculated for free-running animals to occur 4 h after the onset of wheel running activity (CT 12) derived from a regression line fitted to activity onsets on the preceding 7 days. Peptides (0.2 μl, 70 nM, either $Tat_{1–72}$ or $Tat_{\Delta[31–61]}$, randomized) were injected to the SCNs of restrained mice over the course of 1.5 min by removing the stylet and inserting a 28-gauge injector attached to a microsyringe in the dark with the aid of infrared night vision goggles. After 12 days in DD after the first injection, the experiment was repeated a second time with the treatment condition reversed for each animal. Raw phase shifts were calculated as the time difference between the activity onsets on the day of the treatment as extrapolated by regression from the 7 days preceding the injection and the 10 days after the injection (the first 3 days after the injection were discarded). The raw phase shifts were scaled by a factor, τ/24 h, to arrive at the final phase shift in circadian time, where τ is the period exhibited by each mouse before injection. A paired t-test was used to evaluate statistical significance of the phase shifting experiment at an alpha level of 0.05 using Origin 7.0 and Excel.

Reagents. The Tat peptide synthesis and purification procedures have been described elsewhere (22). With the exception of ω-conotoxin GIVA (Bachem, Torrance, CA) and ω-agatoxin IVA (Sigma-Aldrich; Bachem), reagents were purchased from Sigma-Aldrich or Tocris (Ellisville, MO). Reagents were aliquoted and stored at −20° or −80° C (per manufacturers instructions), and diluted in recording solution at the time of the experiment. bafilomycin A_1 and nifedipine were aliquoted in DMSO. All drug delivery tubing, pipette tips, and tubes were silanized with SigmaCoat (Sigma-Aldrich).

RESULTS

$Tat_{1–72}$ resets the circadian clock in vitro. The SCN generates a circadian rhythm of spontaneous action potentials (12). For up to 3 days in vitro, we recorded this rhythm from SCN neurons within the murine brain slice using single-unit extracellular electrodes. The peak of the ensemble rhythm of SCN firing exhibits a stable-phase relationship in tissue isolated from light-entrained rodents, which occurs ~7 h after the onset of the vivarium light-dark cycle [CT 6.84 (mean) ± 0.08 (SE) hr, n = 6; Fig. 1*A*, control]. The first 72 amino acids of Tat ($Tat_{1–72}$), encoded by the first of two exons, are sufficient to confer Glu receptor-mediated membrane depolarization and calcium influx in cultured neurons (15, 30, 41). To determine whether $Tat_{1–72}$ could reset the circadian clock in vitro, we applied $Tat_{1–72}$ to the SCN during the subjective day (CT 7) and night (CT 16 and 22). $Tat_{1–72}$ (7 nM) shifted the phase of the circadian clock, relative to controls, when applied during the early (CT 16, −2.69 ± 0.19 h, n = 8) and late (CT 22, 3.13 ± 0.31 h, n = 5) subjective night but not during the subjective day (CT 7, −0.30 ± 0.07 h, n = 5) (Fig. 1, *A* and *B*). Further, $Tat_{1–72}$-induced phase delays were concentration dependent at CT 16 and more potent (Fig. 1*C*, EC_{50} = 0.312 nM) than the endogenous ligand of light entrainment, Glu (EC_{50} = 1.95 mM).

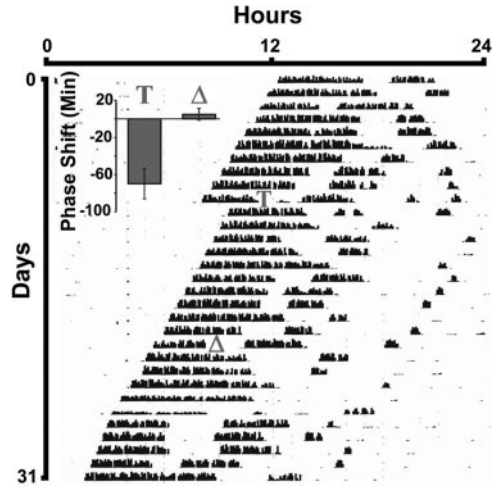

Fig. 2. $Tat_{1–72}$ resets the circadian clock, in vivo. Each free-running mouse received two intraparenchymal SCN injections, spaced 12 days apart, of 70 nM $Tat_{\Delta[31–61]}$ (Δ), and $Tat_{1–72}$ (T) (n = 3) or visa versa (n = 6). An example 31-day actogram (days, ordinate) plotted over 24 h (abscissa) illustrates that $Tat_{1–72}$, but not $Tat_{\Delta[31–61]}$, delays the onset of the circadian rhythm in running wheel behavior, indicated by rightward shift in the daily horizontal raster. The bar graph (inset) demonstrates a significant mean phase delay when $Tat_{1–72}$ (−60.3 ± 14.8 min), but not $Tat_{\Delta[31–61]}$ (3.0 ± 6.8 min), was injected to the SCN at CT 16 [paired t-test (8) = −3.73, n = 9, $P < 0.01$].

Although circadian clock resetting follows the application of $Tat_{1–72}$ in a concentration-dependent manner, it remained unclear whether this effect could be ascribed to this peptide alone. To address this concern, we found that SCN applications of heat-treated $Tat_{1–72}$ (7 nM) at CT 16 did not reset the circadian clock (Fig. 1*D*, HT, 7 nM, 0.01 ± 0.17 h, n = 3). Prior work suggested that the amino acid sequence, 31–61, confers Tat's effect on neurons (13, 30). Application of a $Tat_{1–72}$ peptide, produced under identical conditions, with the amino acid sequence, 31–61, excised did not reset the circadian clock at CT 16 (Fig. 1*D*, $Tat_{\Delta[31–61]}$, 7 nM, −0.22 ± 0.14 h, n = 3).

$Tat_{1–72}$ resets the circadian clock in vivo. The question remained if $Tat_{1–72}$ could shift the phase of the circadian clock in vivo as we have demonstrated in vitro. Therefore, we monitored the circadian rhythm of mouse running wheel behavior in DD. Once these animals reached a steady-state running rhythm in DD, we delivered intraparenchymal injections (0.2 μl) through an implanted cannula of either 70 nM $Tat_{1–72}$ or $Tat_{\Delta[31–61]}$ to the SCN at CT 16 (Fig. 2). Twelve

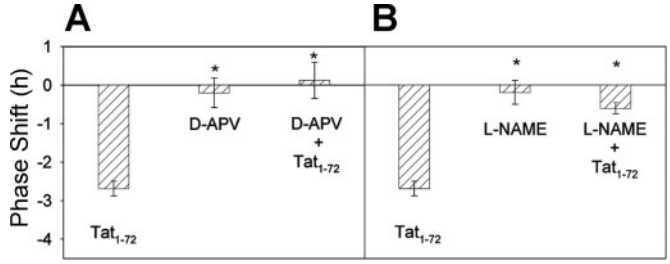

Fig. 3. $Tat_{1–72}$ resets the circadian clock through the *N*-methyl-D-aspartate (NMDA) receptor pathway. *A*: phase delays in the circadian rhythm of spontaneous action potentials generated from the SCN after a 10-min application of $Tat_{1–72}$ (7 nM, -2.69 ± 0.19 h, $n = 8$) at CT 16 in the presence of the NMDA receptor antagonist, 0.1 mM D-APV (applied from CT 15:40–16:10, 0.13 ± 0.47 h, $n = 5$). *B*: Phase delays after a 10-min application of $Tat_{1–72}$ (7 nM, -2.69 ± 0.19 h, $n = 8$) at CT 16 in the presence of the competitive NO synthase blocker, 0.1 μM L-NAME (applied from CT 15:40–16:10, -0.61 ± 0.14 h, $n = 4$). Asterisks indicate statistically significant means comparisons using Scheffé post hoc tests (*$P < 0.05$) relative to the $Tat_{1–72}$ condition, following a one-way ANOVA ($P < 0.0001$).

days later, each animal received a second injection of the other peptide, $Tat_{\Delta[31–61]}$ or $Tat_{1–72}$, respectively. Figure 2, *inset*, demonstrates a mean delay in the onset of running-wheel activity that follows the injection of $Tat_{1–72}$ (-60.3 ± 14.8 min), but not a $Tat_{\Delta[31–61]}$ injection [3.0 ± 6.8 min, paired *t*-test (8) = -3.73, $n = 9$, $P < 0.01$].

$Tat_{1–72}$ resets the circadian clock through the NMDA receptor pathway. The light-like biphasic circadian clock resetting induced by $Tat_{1–72}$ implicates the involvement of the NMDA receptor pathway. To evaluate the role of the NMDA receptor in Tat-induced phase resetting, we applied 7 nM $Tat_{1–72}$ to the SCN brain slice at CT 16 in the presence of a selective and competitive NMDA receptor antagonist D-APV (0.1 mM). Figure 3*A* illustrates that although the blockade of the NMDA receptor does not alter the phase of the circadian rhythm in spontaneous action potentials when applied alone (-0.20 ± 0.38 h, $n = 4$), this action abolished Tat-induced phase shifts (0.13 ± 0.47 h, $n = 5$, $P < 0.05$). Prior evidence suggests that production of NO, downstream of the NMDA receptor, is required for Glu and light-induced phase resetting (11). Competitive blockade of NO synthase, and subsequent NO liberation, with N^G-nitro-L-arginine methyl ester (L-NAME; 1 μM) did not alter the phase of the circadian clock when applied alone (-0.20 ± 0.38 h, $n = 4$) but greatly attenuated $Tat_{1–72}$-induced phase shifts at CT 16 (-0.61 ± 0.14 h, $n = 4$; Fig. 3*B*, $P < 0.05$).

$Tat_{1–72}$ enhances Glu transmission. Although the involvement of the NMDA receptor pathway is supported by the signature circadian time dependence and pharmacology of $Tat_{1–72}$-induced phase resetting, the precise action of Tat remained unclear. To investigate whether $Tat_{1–72}$ directly activates postsynaptic NMDA receptors, or promotes presynaptic release of Glu, we performed whole cell recordings on SCN neurons contained within the hypothalamic brain slice. We examined both the holding currents, as well as NMDA currents evoked by stimulating the optic chiasm with a bipolar electrode, to measure NMDA channel activity before and during the release of Glu, respectively. Figure 4*A* is a representative example of optic-chiasm evoked NMDA currents during bath applications of heat-treated $Tat_{1–72}$ (HT-Tat, -87.5 ± 14.1 pA, 70 nM), $Tat_{1–72}$ (Tat, -170.4 ± 22.8 pA, 70 nM) and D-APV (-22.5 ± 3.08 pA, 100 μM). The normalized peak evoked NMDA currents were significantly increased by $Tat_{1–72}$ com-

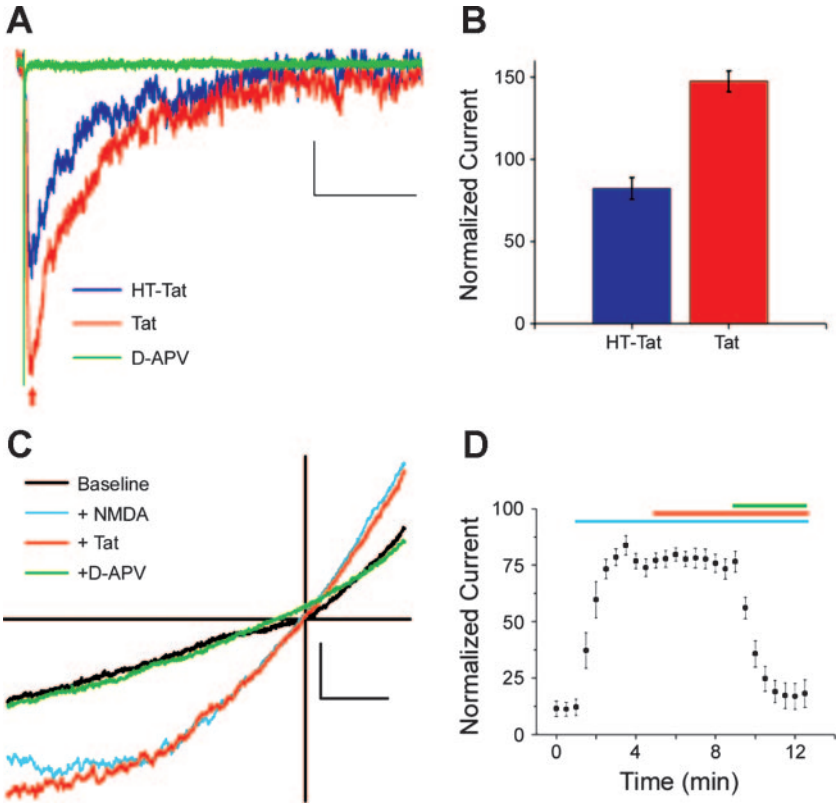

Fig. 4. $Tat_{1–72}$ enhances Glu transmission in the SCN. *A*: NMDA receptor currents isolated in a patch-clamped ventral-lateral SCN neuron subjected to optic chiasm stimulations in the presence of 70-nM heat-treated $Tat_{1–72}$ (HT-Tat, blue), 70 nM $Tat_{1–72}$ (Tat, red), or 100 μM D-APV (D-APV, green). *B*: $Tat_{1–72}$ significantly enhanced the normalized peak NMDA receptor currents, measured at the red arrow, compared with HT-Tat during CT 13–18 [*t* (14) = 5.59, $P < 0.0001$]. The ordinate, labeled normalized current, refers to the percentage of the residual mean evoked-NMDA receptor currents, less the mean evoked current under D-APV conditions, in the treatment and baseline conditions

$$\left(\frac{ENC_{Treatment} - ENC_{DAPV}}{ENC_{Baseline} - ENC_{DAPV}}\right) \times 100\%,$$

where "ENC" is the peak evoked NMDA receptor current and "Treatment" is either $Tat_{1–72}$ or HT-Tat ENCs). *C*: a current-voltage plot derived from a patch-clamped SCN neuron subjected to voltage ramps in bath applications of vehicle solution (baseline, black), with 100 μM NMDA (aqua), and 7 nM $Tat_{1–72}$ (red) and 100 μM D-APV (green). *D*: the mean normalized current (±SE) of ventral-lateral SCN neurons voltage-clamped to −40 mV over time during CT 13–18 under these conditions ($n = 14$ neurons) in the presence of a vehicle bath, supplemented with 7 nM $Tat_{1–72}$ (red), and 100 μM NMDA (green) and 100 μM D-APV (blue). The vertical/horizontal scale bars in (*A*)and (*C*) are 20 pA/500 ms and 35 pA/10 mV, respectively.

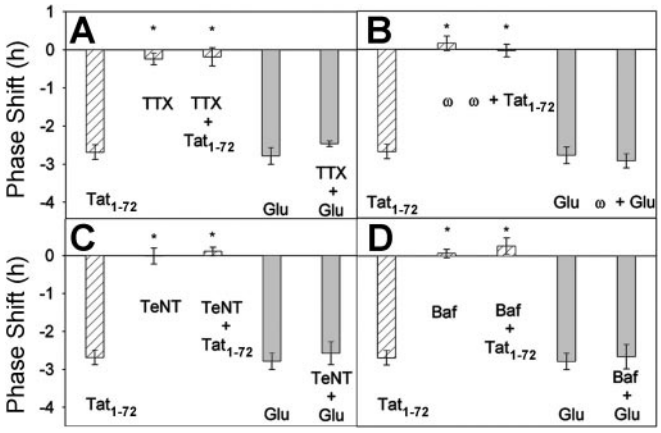

Fig. 5. $Tat_{1–72}$-induced phase resetting requires neurotransmission. *A*: phase delays in the circadian rhythm of spontaneous action potentials recorded from the SCN after applications of $Tat_{1–72}$ (7 nM, 10 min) or Glu (10 mM, 10 min) at CT 16 in the presence of 1 μM TTX applied from CT 15:40–16:10. *B*: Phase delays resulting from a 10-min application of $Tat_{1–72}$ (7 nM) or Glu (10 mM) at CT 16 in the presence of 1 μM ω-conotoxin GIVA (N-type) and 1 μM ω-agatoxin IVA (P/Q-type) (ω) applied from CT 15:40–16:10. *C*: Phase delays following a 10-min application of $Tat_{1–72}$ (7 nM) or Glu (10 mM) at CT 16 in the presence of 2 μg/ml tetanus toxin (TeNT) applied from CT 15:20 to 16:10. *D*: Resulting phase delays after a 10-min application of $Tat_{1–72}$ (7 nM) or Glu (10 mM) at CT 16 in the presence of 1-μM bafilomycin A_1 (Baf) applied from CT 15:10–16:10. Asterisks indicate statistically significant means comparisons using Scheffé post hoc tests (*$P < 0.05$) relative to the $Tat_{1–72}$ condition, following a one-way ANOVA ($P < 0.0001$).

pared with HT-Tat (Fig. 4*B*, $n = 12$, $P < 0.05$). SCN neurons voltage-clamped below 0 mV show increased inward holding currents during applications of NMDA receptor agonists (8, 33). In contrast to $Tat_{1–72}$-enhancement of evoked NMDA currents, the inward holding currents preceding the stimulus did not differ in cells treated with HT-Tat (-66.5 ± 19.9 pA) and $Tat_{1–72}$ (-64.7 ± 19.89 pA), supporting previous findings that $Tat_{1–72}$ does not directly activate the NMDA receptor at nanomolar concentrations (7, 16, 30, 41). To determine whether Tat-induced augmentation of NMDA currents occurs through pre- and/or postsynaptic mechanisms, we compared NMDA currents elicited by voltage ramps after bath applications of NMDA (100 μM) alone and combined with $Tat_{1–72}$ (7 nM) in conditions where evoked synaptic transmission was blocked. The IV plot in Fig. 4*C* illustrates that $Tat_{1–72}$ did not enhance NMDA-induced inward current. This finding is summarized in Fig. 4*D*, showing that $Tat_{1–72}$ did not directly increase NMDA-mediated current in voltage-clamped neurons at −40 mV ($n = 14$, $P > 0.05$).

$Tat_{1–72}$-induced phase resetting requires neurotransmission. At a cellular level, $Tat_{1–72}$ activates NMDA receptors through the enhancement of Glu transmission. However, it remained unclear whether this mechanism could account for $Tat_{1–72}$-induced phase shifts. To test the hypothesis that $Tat_{1–72}$ alters evoked synaptic exocytosis, we incubated the SCN at CT 16 in the sodium channel blocker, TTX (1 μM), and monitored the circadian rhythm of action potentials on subsequent days. As expected from previous reports, TTX did not induce a phase shift when applied alone (-0.24 ± 0.15 h, $n = 3$) (38), but it repressed the ability of $Tat_{1–72}$ to reset the circadian clock (-0.19 ± 0.24 h, $n = 3$, Fig. 5*A*, $P < 0.05$). In contrast, phase delays elicited by direct activation of ionotropic Glu receptors by Glu (10 mM) at CT 16 (-2.78 ± 0.22 h, $n = 4$) were unabated by TTX (-2.46 ± 0.07 h, $n = 3$, $P > 0.05$). Low-voltage-activated calcium channels, P/Q and N-types, mediate presynaptic calcium influx in response to membrane depolarization (6). Accordingly, we evaluated the role of these calcium channels in Tat-induced circadian clock resetting with high concentrations (1 μM) of the channel blockers, ω-conotoxin GIVA (N-type) and ω-agatoxin IVA (P/Q-type). Figure 5*B*, demonstrates that these calcium channel toxins block the ability of $Tat_{1–72}$ to reset the circadian clock (-0.03 ± 0.17 h, $n = 3$, $P < 0.05$) but did not do so when Glu was applied directly (-2.93 ± 0.19 h, $n = 3$, $P > 0.05$). Vesicular fusion occurs when vesicle-localized synaptobrevin binds to presynaptic membrane-bound SNAP-25 and syntaxin. Tetanus toxin cleaves synaptobrevin compromising the vesicular exocytosis (40). When the SCN was incubated in tetanus toxin at CT 16 (2 μg/ml, TeNT, -0.01 ± 0.21 h, $n = 3$), $Tat_{1–72}$ did not reset the circadian rhythm in action potentials (0.11 ± 0.07 h, $n = 3$, Fig. 5*C*, $P < 0.05$). However, direct postsynaptic activation of Glu receptors via Glu did reset this circadian rhythm in the presence of TeNT (-2.57 ± 0.30 h, $n = 3$, Fig. 5*C*, $P > 0.05$). Lastly, vesicular loading of neurotransmitter requires an electrochemical gradient established by the acidification of the vesicle lumen by the proton pump, V-ATPase (24). Bafilomycin A_1 (Baf) is a potent blocker of this pump, which subsequently depletes the vesicular neurotransmitter content (1). Circadian clock resetting in the presence of Baf (0.07 ± 0.11 h, $n = 3$), although possible with exogenous Glu (-2.66 ± 0.32 h, $n = 3$, $P > 0.05$), did not induce phase shifts when $Tat_{1–72}$ was applied (0.26 ± 0.22 h, $n = 3$, Fig. 5*D*, $P < 0.05$).

DISCUSSION

Our work demonstrates, for the first time, that a secreted transcription factor critical in HIV replication can reset the circadian clock in vitro and in vivo. The amino acid sequence encoded by the first exon of the Tat gene (amino acids 1–72) is sufficient to phase shift the circadian pacemaker (Figs. 1 and 2). This exon of Tat requires the amino acid sequence 31–61 (Figs. 1*D* and 2), as it contains critical cell surface binding motifs, the core (amino acids 38–48) and basic (amino acids 48–57) domains that mediate the endocytosis of Tat through the low-density lipoprotein receptor-related protein (21) and through heparan sulfate proteoglycans (21, 43), respectively. Although the role of Tat endocytosis and/or cell surface binding in the enhancement of NMDA receptor currents remains to be clarified, early work suggests that calcium influx and membrane depolarization require both the core and basic regions of Tat (30) and that Tat can only exert these effects when applied extracellularly (7). Future work will identify the extracellular receptor(s) that mediate(s) Tat-induced circadian clock resetting and enhanced Glu release.

The circadian time dependence and pharmacology of $Tat_{1–72}$-induced phase resetting strongly implicate the activation of the NMDA receptor and the subsequent production of NO, the mediators of light entrainment (9, 11). This discovery is consistent with prior work demonstrating the role of NMDA receptors in membrane depolarization, calcium influx, and NO production after Tat application in cortical and hippocampal neurons (15, 17, 20, 34, 41). Our work suggests that the effect of $Tat_{1–72}$ on the light entrainment pathway results from an

enhancement of Glu transmission, as Tat_{1-72}-induced increases in NMDA currents were blocked when evoked neurotransmission was compromised (Fig. 4). These findings were confirmed in our phase-shifting experiments in which direct postsynaptic activation of Glu receptors in the presence of diverse blockers of exocytosis (Fig. 5) did not thwart Glu-induced phase resetting but prevented the ability of Tat_{1-72} to do so. At first glance, these findings are incongruent with prior evidence that Tat acts postsynaptically on the NMDA receptor (15, 41). However, there are important differences in the NMDA receptor composition in the brain areas studied, as well as the concentrations of Tat used. First, kinase-induced enhancement of NMDA receptor currents occurs only for NMDA receptors composed of subunits NR2A or NR2B but not NR2C or NR2D (28). This difference in subunit composition and phosphorylation potential may explain why nanomolar concentrations of Tat could potentiate currents in hippocampal/cortical neurons, which are enriched with NR2A and NR2B subunits, but not in SCN neurons where NR2C subunits predominate (25, 45). Secondly, prior reports (41) suggest that micromolar concentrations of Tat are required to evoke inward currents through a direct NMDA receptor interaction that is insensitive to Glu- and glycine-site antagonists. Since the concentrations required to achieve this effect are substantially greater than the nanomolar concentrations of Tat used to induce phase shifts and that the effects presented here are D-APV sensitive, we do not believe that a direct interaction with the NMDA receptor underlies Tat-induced phase shifts. From the evidence outlined here, we believe that NMDA receptor activation depends on neurotransmission in the SCN rather than through a postsynaptic mechanism, as implicated in other brain regions.

Light entrainment is a process where the circadian pacemaker synchronizes to the environmental light-dark cycle as a consequence of phase shifts induced by daily light exposure (36). This process is mediated by Glu release from retinal ganglion afferents that innervate the SCN (14). The HIV protein, Tat, can lead to NMDA-receptor-dependent phase shifts, independent of light, by enhancing evoked Glu release from intrinsic and afferent SCN synapses. During lentiviral infection, HIV-Tat may alter light entrainment, downstream of light-induced Glu release, by resetting the circadian clock in a pattern dictated by the disease progression in addition to the light-dark cycle. Thus this pathological resetting of the circadian clock may disrupt the natural process of light entrainment and account for the unusual and varying phase relationships of the circadian rhythms in body temperature, movement, and circulating immune cells seen during lentiviral infection (5–9).

ACKNOWLEDGMENTS

We thank P. Ray for preparing the Tat peptides; J. Waataja for software programming; C. S. Colwell, H. S. Fox, S. J. Henriksen, P. K. Peterson for their advice and support and N. C. Connors for comments on this paper.

GRANTS

This work was supported by National Institutes of Health Grant NS-047014, DA-09924, DA-04381, and a National Science Foundation IGERT Fellowship 9870633.

REFERENCES

1. **Bezzi P, Domercq M, Brambilla L, Galli R, Schols D, De Clercq E, Vescovi A, Bagetta G, Kollias G, Meldolesi J, and Volterra A.** CXCR4-activated astrocyte glutamate release via TNFα: amplification by microglia triggers neurotoxicity. *Nature* 4: 702–710, 2001.
2. **Bourin P, Mansour I, Doinel C, Roue R, Rouger P, and Levi F.** Circadian rhythms of circulating NK cells in healthy and human immunodeficiency virus-infected men. *Chronobiol Int* 10: 298–305, 1993.
3. **Bruce-Keller AJ, Chauhan A, Dimayuga FO, Gee J, Keller JN, and Nath A.** Synaptic transport of human immunodeficiency virus-Tat protein causes neurotoxicity and gliosis in rat brain. *J Neurosci* 23: 8417–8422, 2003.
4. **Burudi EM and Fox HS.** Simian immunodeficiency virus model of HIV-induced central nervous system dysfunction. *Adv Virus Res* 56: 435–468, 2001.
5. **Chang HC, Samaniego F, Nair BC, Buonaguro L, and Ensoli B.** HIV-1 Tat protein exits from cells via a leaderless secretory pathway and binds to extracellular matrix-associated heparan sulfate proteoglycans through its basic region. *AIDS* 11: 1421–1431, 1997.
6. **Chen G and van den Pol AN.** Presynaptic GABAB autoreceptor modulation of P/Q-type calcium channels and GABA release in rat suprachiasmatic nucleus neurons. *J Neurosci* 18: 1913–1922, 1998.
7. **Cheng J, Nath A, Knudsen B, Hochman S, Geiger JD, Ma M, and Magnuson DS.** Neuronal excitatory properties of human immunodeficiency virus type 1 Tat protein. *Neuroscience* 82: 97–106, 1998.
8. **Colwell CS.** NMDA-evoked calcium transients and currents in the suprachiasmatic nucleus: gating by the circadian system. *Eur J Neurosci* 13: 1420–1428, 2001.
9. **Colwell CS, Foster RG, and Menaker M.** NMDA receptor antagonists block the effects of light on circadian behavior in the mouse. *Brain Res* 554: 105–110, 1991.
10. **Darko DF, McCutchan JA, Kripke DF, Gillin JC, and Golshan S.** Fatigue, sleep disturbance, disability, and indices of progression of HIV infection. *Am J Psychiatry* 149: 514–520, 1992.
11. **Ding JM, Chen D, Weber ET, Faiman LE, Rea MA, and Gillette MU.** Resetting the biological clock: mediation of nocturnal circadian shifts by glutamate and NO. *Science* 266: 1713–1717, 1994.
12. **Gillette MU, Medanic M, McArthur AJ, Liu C, Ding JM, Faiman LE, Weber ET, Tcheng TK, and Gallman EA.** Intrinsic neuronal rhythms in the suprachiasmatic nuclei and their adjustment. *Ciba Found Symp* 183: 134–144, 1995.
13. **Gurwell JA, Nath A, Sun Q, Zhang J, Martin KM, Chen Y, and Hauser KF.** Synergistic neurotoxicity of opioids and human immunodeficiency virus-1 Tat protein in striatal neurons in vitro. *Neuroscience* 102: 555–563, 2001.
14. **Hannibal J.** Neurotransmitters of the retino-hypothalamic tract. *Cell Tissue Res* 309: 73–88, 2002.
15. **Haughey NJ, Holden CP, Nath A, and Geiger JD.** Involvement of inositol 1,4,5-trisphosphate-regulated stores of intracellular calcium in calcium dysregulation and neuron cell death caused by HIV-1 protein tat. *J Neurochem* 73: 1363–1374, 1999.
16. **Haughey NJ, Nath A, Mattson MP, Slevin JT, and Geiger JD.** HIV-1 Tat through phosphorylation of NMDA receptors potentiates glutamate excitotoxicity. *J Neurochem* 78: 457–467, 2001.
17. **Hayman M, Arbuthnott G, Harkiss G, Brace H, Filippi P, Philippon V, Thomson D, Vigne R, and Wright A.** Neurotoxicity of peptide analogs of the transactivating protein Tat from Maedi-Visna virus and human immunodeficiency virus. *Neuroscience* 53: 1–6, 1993.
18. **Kaul M, Garden GA, and Lipton SA.** Pathways to neuronal injury and apoptosis in HIV-associated dementia. *Nature* 410: 988–994., 2001.
19. **Kim BO, Liu Y, Ruan Y, Xu ZC, Schantz L, and He JJ.** Neuropathologies in transgenic mice expressing human immunodeficiency virus type 1 Tat protein under the regulation of the astrocyte-specific glial fibrillary acidic protein promoter and doxycycline. *Am J Pathol* 162: 1693–1707, 2003.
20. **Kruman II, Nath A, and Mattson MP.** HIV-1 protein Tat induces apoptosis of hippocampal neurons by a mechanism involving caspase activation, calcium overload, and oxidative stress. *Exp Neurol* 154: 276–288, 1998.
21. **Liu Y, Jones M, Hingtgen CM, Bu G, Laribee N, Tanzi RE, Moir RD, Nath A, and He JJ.** Uptake of HIV-1 tat protein mediated by low-density lipoprotein receptor-related protein disrupts the neuronal metabolic balance of the receptor ligands. *Nat Med* 6: 1380–1387, 2000.
22. **Ma M and Nath A.** Molecular determinants for cellular uptake of Tat protein of human immunodeficiency virus type 1 in brain cells. *J Virol* 71: 2495–2499, 1997.

23. **Martini E, Muller JY, Doinel C, Gastal C, Roquin H, Douay L, and Salmon C.** Disappearance of CD4-lymphocyte circadian cycles in HIV-infected patients: early event during asymptomatic infection. *AIDS* 2: 133–134, 1988.
24. **Maycox PR, Deckwerth T, Hell JW, and Jahn R.** Glutamate uptake by brain synaptic vesicles. Energy dependence of transport and functional reconstitution in proteoliposomes. *J Biol Chem* 263: 15423–15428, 1988.
25. **Mikkelsen JD, Larsen PJ, and Ebling FJ.** Distribution of N-methyl D-aspartate (NMDA) receptor mRNAs in the rat suprachiasmatic nucleus. *Brain Res* 632: 329–333, 1993.
26. **Miller RJ and Meucci O.** AIDS and the brain: is there a chemokine connection? *Trends Neurosci* 22: 471–479, 1999.
27. **Moore RY.** Circadian rhythms: basic neurobiology and clinical applications. *Annu Rev Med* 48: 253–266, 1997.
28. **Mori H, Yamakura T, Masaki H, and Mishina M.** Involvement of the carboxyl-terminal region in modulation by TPA of the NMDA receptor channel. *Neuroreport* 4: 519–522, 1993.
29. **Nath A and Geiger J.** Neurobiological aspects of human immunodeficiency virus infection: neurotoxic mechanisms. *Prog Neurobiol* 54: 19–33., 1998.
30. **Nath A, Psooy K, Martin C, Knudsen B, Magnuson DS, Haughey N, and Geiger JD.** Identification of a human immunodeficiency virus type 1 Tat epitope that is neuroexcitatory and neurotoxic. *J Virol* 70: 1475–1480., 1996.
31. **Norman SE, Resnick L, Cohn MA, Duara R, Herbst J, and Berger JR.** Sleep disturbances in HIV-seropositive patients. *JAMA* 260: 922, 1988.
32. **Opp MR, Rady PL, Hughes TK, Cadet P, Tyring SK, Smith EM.** Human immunodeficiency virus envelope glycoprotein 120 alters sleep and induces cytokinemRNA expression in rats. *Am J Physiol Regul Integr Comp Physiol* 271: R963–R970, 1996.
33. **Pennartz CM, Hamstra R, and Geurtsen AM.** Enhanced NMDA receptor activity in retinal inputs to the rat suprachiasmatic nucleus during the subjective night. *J Physiol* 532: 181–194., 2001.
34. **Perez A, Probert AW, Wang KK, and Sharmeen L.** Evaluation of HIV-1 Tat induced neurotoxicity in rat cortical cell culture. *J Neurovirol* 7: 1–10, 2001.
35. **Philippon V, Vellutini C, Gambarelli D, Harkiss G, Arbuthnott G, Metzger D, Roubin R, and Filippi P.** The basic domain of the lentiviral Tat protein is responsible for damages in mouse brain: involvement of cytokines. *Virology* 205: 519–529., 1994.
36. **Pittendrigh CS and Daan S.** A functional analysis of circadian pacemakers in nocturnal rodents IV: entrainment: pacemaker as clock. *J Comp Physiol A* 106: 291–331, 1976.
37. **Prospero-Garcia O, Herold N, Phillips TR, Elder JH, Bloom FE, and Henriksen SJ.** Sleep patterns are disturbed in cats infected with feline immunodeficiency virus. *Proc Natl Acad Sci USA* 91: 12947–12951, 1994.
38. **Prosser RA, Heller HC, and Miller JD.** Serotonergic phase shifts of the mammalian circadian clock: effects of tetrodotoxin and high Mg^{2+}. *Brain Res* 573: 336–340, 1992.
39. **Sanchez-Alavez M, Criado J, Gomez-Chavarin M, Jimenez-Anguiano A, Navarro L, Diaz-Ruiz O, Galicia O, Sanchez-Narvaez F, Murillo-Rodriguez E, Henriksen SJ, Elder JH, and Prospero-Garcia O.** HIV- and FIV-derived gp120 alter spatial memory, LTP, and sleep in rats. *Neurobiol Dis* 7: 384–394, 2000.
40. **Schiavo G, Benfenati F, Poulain B, Rossetto O, Polverino de Laureto P, DasGupta BR, and Montecucco C.** Tetanus and botulinum-B neurotoxins block neurotransmitter release by proteolytic cleavage of synaptobrevin. *Nature* 359: 832–835, 1992.
41. **Song L, Nath A, Geiger JD, Moore A, and Hochman S.** Human immunodeficiency virus type 1 Tat protein directly activates neuronal N-methyl-D-aspartate receptors at an allosteric zinc-sensitive site. *J Neurovirol* 9: 399–403., 2003.
42. **Swoyer J, Rhame F, Hrushesky W, Sackett-Lundeen L, Sothern R, Gale H, and Haus E.** Circadian rhythm alteration in HIV-infected subjects. *Prog Clin Biol Res* 437–449, 1990.
43. **Tyagi M, Rusnati M, Presta M, and Giacca M.** Internalization of HIV-1 tat requires cell surface heparan sulfate proteoglycans. *J Biol Chem* 276: 3254–3261, 2001.
44. **Vagnucci AH and Winkelstein A.** Circadian rhythm of lymphocytes and their glucocorticoid receptors in HIV-infected homosexual men. *J Acquir Immune Defic Syndr Hum Retrovirol* 6: 1238–1247, 1993.
45. **Watanabe M, Inoue Y, Sakimura K, and Mishina M.** Developmental changes in distribution of NMDA receptor channel subunit mRNAs. *Neuroreport* 3: 1138–1140, 1992.